energy&fuels

Article

Cite This: Energy Fuels 2019, 33, 8946−8953

pubs.acs.org/EF

Adsorption Kinetics of CO_2 on a Reconstructed Calcite Surface: An Experiment-Simulation Collaborative Method

Lin Tao,[†] Junchen Huang,[†] Xitao Yin,*[,†] Qi Wang,*[,†] Zhi Li,[†] Guocheng Wang,[†] and Baoyu Cui[‡]

[†]The Key Laboratory of Chemical Metallurgy Engineering of Liaoning Province, University of Science and Technology Liaoning, Anshan, Liaoning Province 114051, China

[‡]School of Resources and Civil Engineering, Northeastern University, Shenyang, Liaoning Province 110819, China

ABSTRACT: Because the CO_2−calcite interface is of major importance in various environments and the energy industry, an accurate description of the adsorption kinetics of CO_2 is critical for understanding the adsorption mechanisms involved. In this study, a new electrochemical method was implemented to unravel the adsorption kinetics of CO_2 on a reconstructed calcite surface. In addition, an atomic simulation was used to provide details of the adsorbed interface. The results showed that the reconstructed calcite surface had different electrical conductivity under various conditions, which was attributed to differences in band gap values. The CO_2 adsorption process on the reconstructed calcite surface was characterized by a change in electrical conductivity. Consequently, the adsorption rate constant at different temperatures and the energy barrier to be overcome in the gas adsorption process were obtained, with values of 0.0272−0.0412 s^{-1} and 5.51 kJ/mol, respectively. This experimental result was well verified by molecular dynamics simulation. This study proved that the electrical conductivity of the material surface can accurately and quickly reflect the gas adsorption process, and the simulation method provided more details of the adsorption behavior at the gas−solid interface.

1. INTRODUCTION

Calcite is one of the most important minerals in nature. The calcite surface and CO_2 adsorbed interface are extensive involved in a variety of biological and energy industrial processes under various conditions such as biomineralization,[1] geosequestration of CO_2,[2] enhanced oil recovery,[3,4] and flue gas separation.[5] Under complex conditions, it is difficult to study CO_2 adsorption on a calcite surface by traditional experimental methods.[6,7] Most studies have been based on molecular dynamics (MD) simulation methods to provide thermodynamic feasibility.

So far, some typical studies on CO_2 adsorption on calcite surfaces have been reported. For instance, Wang et al.[8] found through MD simulation that CO_2 molecules can form an apparently adsorbed layer on a calcite surface. Sun et al.[3,9] used an MD simulation method to investigate the competitive adsorption of CO_2 and CH_4 on a calcite surface, proving that CO_2 molecules have a much higher capacity than CH_4 to be adsorbed onto calcite surfaces. Besides this, Economou's group[4,7,10] focused on the thermodynamic properties of CO_2 adsorption as well as the anisotropic behavior of the transport properties of CO_2 confined by a calcite surface using classical MD simulation. Tao et al.[11] reported the effect of various temperatures on the interface adsorption behavior of CO_2 molecules. In particular, the calcite surface can also be used to achieve CO_2 capture from flue gas.[5] Given that calcite is an abundant and widely distributed mineral on Earth, calcite-based substances are a promising alternative to replace other materials and thus to weaken the greenhouse effect. The feasibility of these adsorption processes has been well demonstrated by MD simulation. Significantly, the adsorption processes are attributed to strong electrostatic interactions between CO_2 and the calcite surface.[4,10−12] For sensitive materials,[13,14] gas adsorption can change surface electronic properties, including electrical conductivity and electronic structure. From the perspective of electronic properties, this approach could be used to understand the adsorption mechanism of gas on the material surface.

Therefore, it is reasonable to speculate that the electrical properties of a calcite surface should be affected by electrostatic interactions in the CO_2 adsorption process. However, studies of the electronic properties of calcite surfaces and CO_2-adsorbed surfaces are rare. In addition, under complex high-temperature conditions, it is still a challenging problem to study the adsorption of fluids on material surfaces, let alone to understand the kinetic behavior of adsorption in depth.

In previous work by the authors, the gas-sensing mechanism was based on changes in the sensing signal caused by gas adsorption. Yin et al.[15] characterized the adsorption properties of CO on a SnO_2 surface by measuring surface conductivity. Furthermore, the adsorption mechanism of low concentration H_2 on the SnO_2 surface was investigated through conductivity variation patterns.[16] Liu et al.[17] revealed that a directly proportional relationship between the limiting current and the oxygen sensing performance of the solid electrolyte could be successfully verified by surface electrical conductivity. However, the opposite process, that is, using the sensing signal to study adsorption behavior, has rarely been reported. Therefore, in this study, a simple new method was developed to measure the effect of CO_2 adsorption on the electrical conductivity of a calcite surface. It was expected that the adsorption process of

Received: May 31, 2019
Revised: July 30, 2019
Published: August 12, 2019

DOI: 10.1021/acs.energyfuels.9b01771
Energy Fuels 2019, 33, 8946−8953

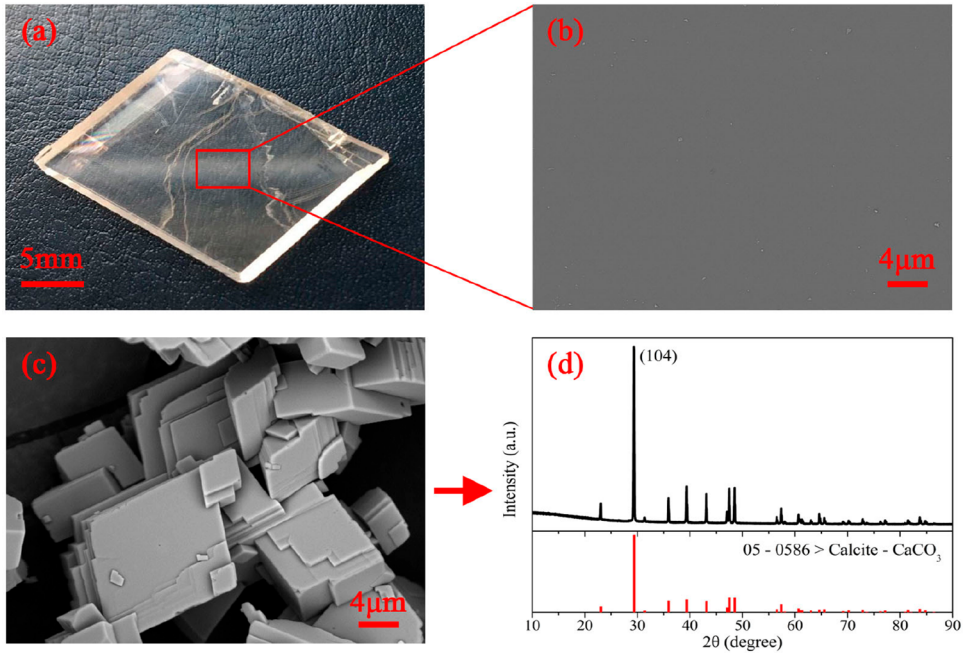

Figure 1. (a) Single calcite crystal; (b) SEM of the calcite crystal surface; (c) SEM of calcite powders for XRD detection; and (d) XRD of calcite powders.

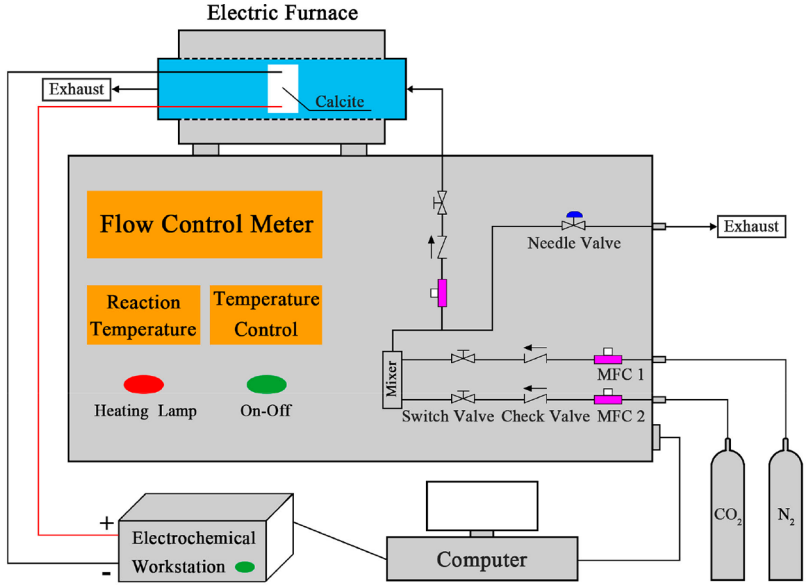

Figure 2. Schematic diagram of the experiment.

CO_2 on a calcite surface could be represented by the electrical conductivity of the surface. To the best of the authors' knowledge, few experimental studies have been reported in the literature on the electrical properties of calcite surface during CO_2 adsorption at different temperatures.

In this study, a new electrochemical method was implemented to measure the electrical current of a pure calcite surface and a CO_2 adsorbed surface in situ at different temperatures. Furthermore, the density functional theory (DFT) and MD simulation were used to unravel the details of surface and interface phenomena. As expected, synergistic integration of experimental and simulation approaches reveals more details of kinetic adsorption behavior and explains calcite surface conduction in terms of electronic structure. Importantly, the energy barrier to be overcome in the gas adsorption process was obtained and then well validated by MD simulation. This work provides a new physicochemical view to understand the gas−solid interface (adsorption, catalysis, sensor, etc.) according to the electrical properties of material surfaces.

2. EXPERIMENTAL SECTION

2.1. Preparation and Characterization of Materials. The (104) cleave surface was cut from an optical quality calcite crystal (Iceland spar), because it is the most stable thermodynamically crystallographic plane and is exposed to nature,[18−21] as shown in Figure 1. Then, the sample was checked by field emission scanning electron microscopy (FESEM, ZEISS-ΣIGMA HD) and X-ray diffraction (XRD) (PANalytical X, RigakuD/max-Ra with Cu Kα

DOI: 10.1021/acs.energyfuels.9b01771
Energy Fuels 2019, 33, 8946−8953

radiation, λ = 0.15418 nm). It was ascertained that the calcite surface was smooth and that the calcite phase was pure.

2.2. Apparatus. All electrochemical measurements were obtained in a custom-designed experimental apparatus consisting of a gas mass flow controller (MFC), a tube electric furnace (temperature range of 298−1273 K; tube diameter of 38 mm), dedicated temperature-control software (computer), and an electrochemical workstation (CHI660E, Chenhua Instruments, Inc., China), as shown in Figure 2.

2.3. Electrochemical Measurement. First, the platinum electrodes were placed on the same surface of the calcite crystal, and the assemblage was inserted into an electrical furnace. The sample was heated to a target temperature (298, 373, 423, 473, 523, 623, and 673 K) at a temperature increase rate of 5 K/min with N_2 protection (99.99%, 500 mL/min). The time of each measurement was fixed at 1200 s. The CO_2 gas (99.99%, 500 mL/min) was injected into the test tube under the control of the mass flow apparatus at 600 s. The electrical currents of the calcite surface in both N_2 gas and binary mixture gas were measured by an electrochemical workstation. During the experiment, *i-t* curve measurements under constant voltage (U = 5 V) were obtained. The experimental result for each electrochemical measurement contained three independent experiments. The repeatability of the experiments was acceptable.

2.4. Computational Models. Figure 3 shows the initial multilayered adsorption structure and the parameters of the gas−

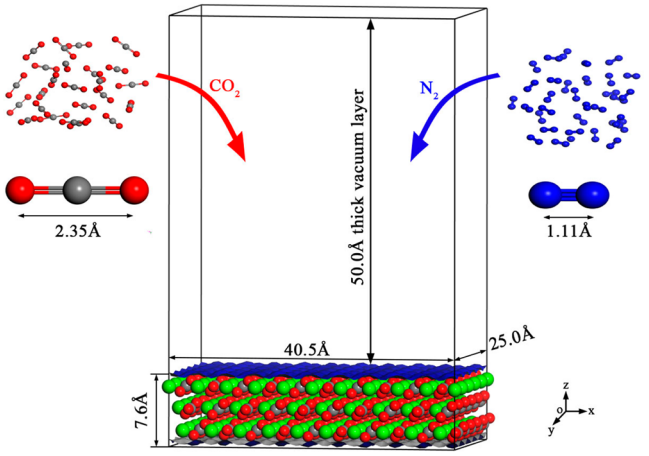

Figure 3. Model of gas adsorption on the calcite (104) surface. The atomic designations are Ca (green), C (gray), N (blue), and O (red).

calcite system. Binary mixture gas was composed of CO_2 and N_2 in a 1:1 ratio. The top layer of the calcite surface was allowed to relax, but the rest of the atoms were considered rigid in all MD simulations.[11,22] Because the fixed atoms are separately thermostated and are not bonded to the surface atoms, fixing their positions has a negligible impact on the simulation results.[6,23] A better three-site model with three partial charges was introduced for CO_2, whereas the two-site model with LJ parameters was used to calculate the neutral N_2.[24−26] The configurations of the gas molecules (CO_2 and N_2) were optimized and were consistent with literature results.[24−26]

2.5. Simulation Details. The Dmol^3 module[27,28] was used to calculate the band gap of the surface structure, within the framework of the DFT. The exchange-correlation potential was considered in the generalized gradient approximation (GGA),[29] combined with the Perdew−Wang (PW91) exchange functional.[30] The default value of temperature calculated by the Dmol^3 module is 0 K. To calculate the band gaps of the adsorption systems at different temperatures, MD simulation was first used to obtain the structure of each adsorption system at different temperatures, and DFT was applied to calculate the band gap of each surface structure.

The Forcite module of Materials Studio and the COMPASS force field[31,32] were employed to simulate CO_2−calcite interface adsorption. This is the first ab initio force field and has been validated to be capable of accurately predicting structural and thermophysical properties for a broad range of organic and inorganic substances,[31,32] such as N_2, CO_2, and calcite.[3,5,8,33] The COMPASS force field consists of bonded and nonbonded interactions. Bonded interactions include bond stretching, angular bending, dihedral angle torsion, out-of-plane interactions, and cross terms. Nonbonded interactions are composed of the long-range electrostatic interaction and the short-range van der Waals interaction, which were calculated by Coulombic interactions and the Lennard−Jones 9−6 function, respectively. The Coulombic interactions were evaluated by the Ewald method, whereas the Lennard−Jones 9−6 interactions were calculated by the atom-based method. All simulations were carried out for a constant number, constant volume, and constant temperature (NVT) ensemble. The temperature was controlled using the Nose thermostat. The initial velocity of the gas molecules was identical to the Boltzmann distribution according to the assumption that the time average is equivalent to the ensemble average.[6] Each MD simulation required 5 × 10^6 calculation steps. The time step and the total simulation time were set to 1 fs and 5 ns, respectively. The first 4 ns were used for equilibration, and the last 1 ns of the MD simulation was used for data analysis. The full trajectory was recorded, and the frames were output every 500 steps. The statistical analysis for each adsorption structure consisted of three independent runs of 1 ns after equilibration.

3. RESULTS AND DISCUSSION

3.1. Electrical Current Response of Calcite Surface. Figure 4 shows the electrical current variation curves of the

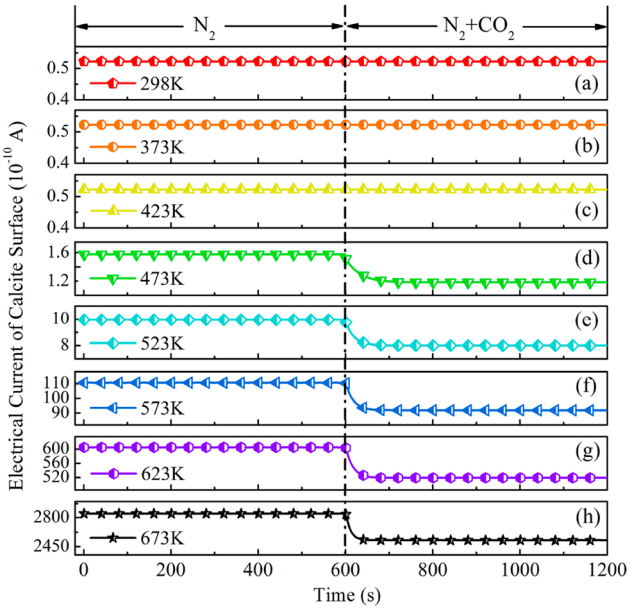

Figure 4. Electrical current of a calcite surface at different temperatures.

CO_2 adsorption process that were obtained at different temperatures. There was no clear change in the electrical current after CO_2 adsorption below 473 K. When the temperature was higher than 473 K, a significant decrease in electrical current was observed, which was caused by CO_2 adsorption. This phenomenon can be attributed to electrostatic interaction between CO_2 and the calcite surface,[10,34] which changed the charge state of the surface. The electrical conductivities of both pure calcite surfaces (N_2-surface) and adsorbed surfaces (CO_2-surface) were both enhanced with increasing temperature.

DOI: 10.1021/acs.energyfuels.9b01771
Energy Fuels 2019, 33, 8946−8953

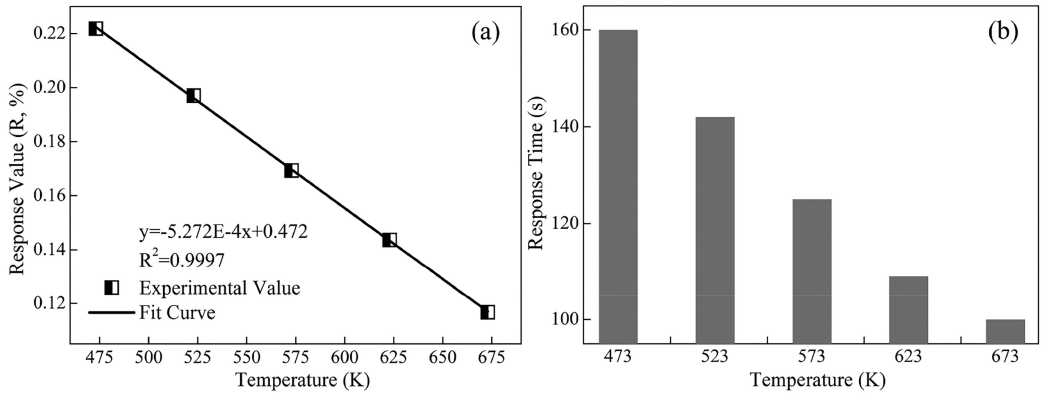

Figure 5. (a) Linear relationship between the response value of a calcite surface to CO_2 and temperature. (b) Response time of a calcite surface to CO_2 at different temperatures.

To quantify the effect of CO_2 on the electrical current in a calcite surface in the temperature range of 473−673 K, the concept of response value is introduced. The response value was defined as follows:

$$R = (I_{pure} - I_{ads})/I_{pure} \quad (1)$$

where R is the response value of the calcite surface to CO_2 (%), I_{pure} is the electrical current of pure surface (A), and I_{ads} is the electrical current of adsorbed surface (A). As shown in Figure 5 (a), the response value of calcite surface to CO_2 decreased with increasing temperature and was linearly correlated with temperature according to the fitted curve. It can be concluded that CO_2 adsorption on a calcite surface followed a first-order kinetic model. From Figure 5(b), the response time of a calcite surface to CO_2 at high temperature was faster than at low temperature. This indicated that the higher the temperature was, the greater the surface activity of the calcite was.

3.2. Reconstructed Surfaces and Electrical Structure of Calcite. Interestingly, calcite is an insulator with a band gap of 6.0 ± 0.35 eV at 0 K.[35] However, the surface electrical conductivity can be detected at a certain temperature and is affected by CO_2 adsorption. First, this suggested that the calcite crystal had special semiconducting properties at high temperature, which is consistent with the literature.[36] Second, it proved that calcite crystals provided almost entirely surface-layer conduction. This conduction may be directly related to the fact that the top layer of calcite was largely reconstructed.[22,37,38]

Because the surface is the termination of the 3D periodicity of the bulk crystal, it has a large number of dangling bonds and can become unstable. To reduce surface free energy, or lattice stress, the surface atoms were displaced from their original positions at nanoscale, and the symmetry of the resulting structure was different from that of the bulk crystal.[39−41] Consequently, the reconstructed surface had different surface properties (conductivity, magnetic, and optical). In addition, the reconstructed surface is also affected by temperature and by adsorption of gas molecules, resulting in a change in the surface electronic properties. However, it is difficult to achieve this surface structure and electronic properties at high temperature in experiments. Hence, in this study, MD simulation was first used to obtain the reconstructed surfaces, including the pure calcite surface and the adsorbed surface, at different temperatures. Then, the electrical properties of the reconstructed surface were calculated by DFT.

Figure 6 shows reconstructions of a pure calcite surface and an adsorbed surface at different temperatures. The reconstructed surface was different from the bulk phase structure and is markedly affected by temperature. The simulation results confirmed the description of the reconstructed surface very well. When CO_2 molecules were adsorbed on the calcite surface, the reconstruction remained. However, it was difficult to distinguish between a pure and an adsorbed surface from the geometric structure of the surface. For this reason, the DFT was used in this study to calculate the band gap of all the surface structures in Figure 6 because the band gap represented the conductivity of a material. In Figure 7, the calculated results showed that the band gap of both pure and adsorbed surfaces decreased with rising temperature, leading to enhanced surface conductivity. Furthermore, when the temperature was below 473 K, the band gap of the calcite surface was relatively wide. This results in low electrical conductivity that was not enough to generate an apparent electrical current. When the temperature exceeded 473 K, the surface conductivity was enhanced because of the sudden decrease in band gap. Hence, the effect of CO_2 on surface

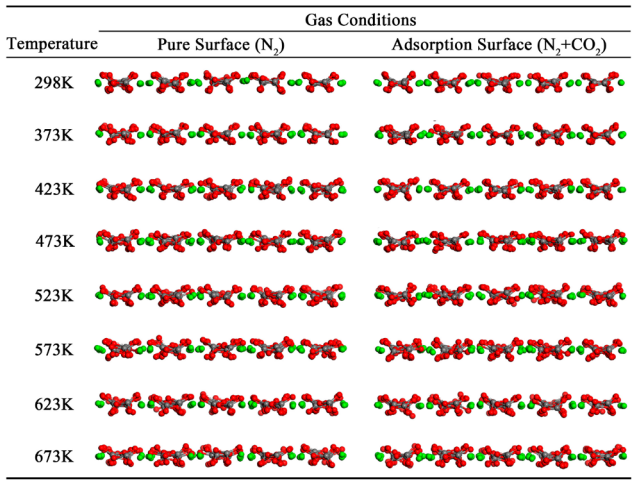

Figure 6. Structures of a reconstructed calcite surface at different temperatures viewed from the ox vector. The atomic designations are Ca (green), C (gray), N (blue), and O (red).

DOI: 10.1021/acs.energyfuels.9b01771
Energy Fuels 2019, 33, 8946−8953

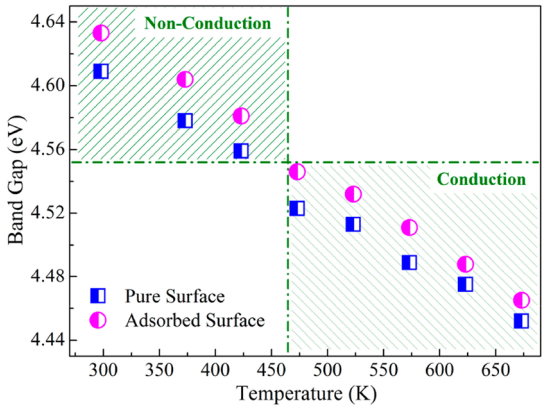

Figure 7. Trends of the band gap of a pure calcite surface and an adsorbed surface with temperature.

electrical current was detected. In the light of Figure 7, it can be stated that the difference in band gap between pure and adsorbed surfaces decreased with rising temperature. This trend was a good verification of the results shown in Figure 5(a).

3.3. Interface Adsorption of CO_2. Although the number of CO_2 molecules flowing through the surface was the same, the response value of a calcite surface varied with temperature. This indicated that the response value of a calcite surface had a certain correlation with the amount of CO_2 adsorbed. Under high-temperature conditions, it was difficult to study CO_2 adsorption on a calcite surface by traditional experimental methods.[6−8] Simulations now routinely help unravel the details of the interface behavior of fluids flowing across chemically structured surfaces.[42] Hence, it was necessary to obtain information about CO_2 adsorption on calcite surfaces by MD simulation.

The first step was to simulate the detailed adsorption structure of CO_2 on a calcite surface at 473 K. Figure 8 shows

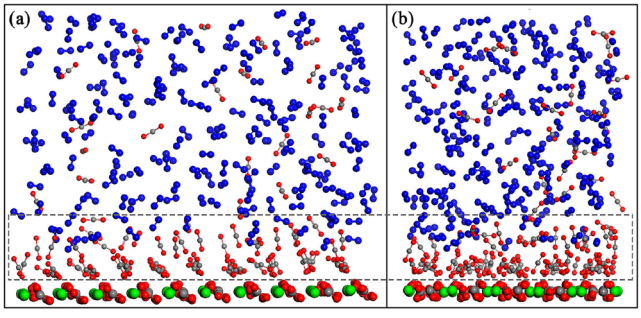

Figure 8. Snapshot of CO_2 adsorption structure on a reconstructed calcite surface at 473 K viewed from the oy vector (a) and the ox vector (b). The atomic designations are Ca (green), C (gray), N (blue), and O (red).

the formation of the CO_2 interface near the reconstructed calcite surface. The CO_2−calcite system was equilibrated until the CO_2 distribution became constant with time. The CO_2 molecules had an apparent adsorption layer close to the reconstructed calcite surface, and CO_2 molecules were adsorbed onto the surface at the sites of Ca ions in a highly oriented arrangement. The angle of CO_2 molecules with respect to the (104) surface was approximately 40°−45°, which was close to the angle of the carbonate group plane relative to the (104) surface. In addition, CO_2 molecules occupying well-defined positions with respect to the crystal surface could be attributed to electrostatic interaction between the Ca ions in calcite and the O atoms in CO_2. On the contrary, the N_2 molecules had no distinct adsorption layer. N_2 was sequestered from the surface by CO_2. As mentioned above, CO_2 molecules preferred to adsorb on the calcite surface, whereas N_2 molecules showed a relatively uniform distribution in the upper part of the calcite surface.

Second, based on the results shown in Figure 8, the differences in surface density of CO_2 adsorbed on the calcite surface at different temperatures were compared. Because the surface density of gas is equivalent to the amount of gas adsorbed, the surface density reflects not only the adsorption amount but also the adsorption structure. The surface density was calculated as the number of CO_2 molecules adsorbed on the calcite surface divided by the area of the calcite surface. The surface density of Ca ions on the calcite surface was also calculated, and the relationship between the surface density of adsorbed CO_2 and the available Ca sites on the calcite surface was analyzed. The results are shown in Figure 9; the surface

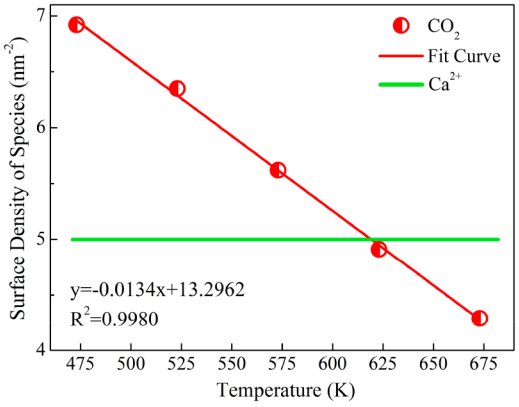

Figure 9. Surface density of CO_2 and Ca^{2+} as a function of temperature.

density of CO_2 gas decreases with rising temperature and is linearly correlated with temperature according to the fitted curve. The surface density of Ca ions remains constant. At approximately 623 K, the density of CO_2 was almost equal to that of Ca ions, indicating that adsorption should be monolayer at this moment, that is, each Ca ion was bound to an O atom in CO_2 through electrostatic interaction. When the temperature was lower than 573 K, the CO_2 molecules on the calcite surface should exhibit a double-layer adsorption structure because the surface density of CO_2 had exceeded the surface density of the Ca ion. This result is clearly shown in Figure 8.

3.4. Adsorption Kinetic. *3.4.1. Pseudo-First-Order Kinetic Model.* According to Figures 5(a) and 9, the response value of a calcite surface to CO_2 and the surface density of CO_2 were linearly related to temperature. Therefore, when the surface density of CO_2 was converted to the amount of CO_2 adsorbed, the relationship between the response value and the amount adsorbed was linear, as shown in Figure 10(a). This strongly indicated that the response value of a calcite surface to CO_2 represented the amount of CO_2 adsorbed. In other words, the process of electrical current change was the process of CO_2 adsorption. Consequently, the electrical current change

DOI: 10.1021/acs.energyfuels.9b01771
Energy Fuels 2019, 33, 8946−8953

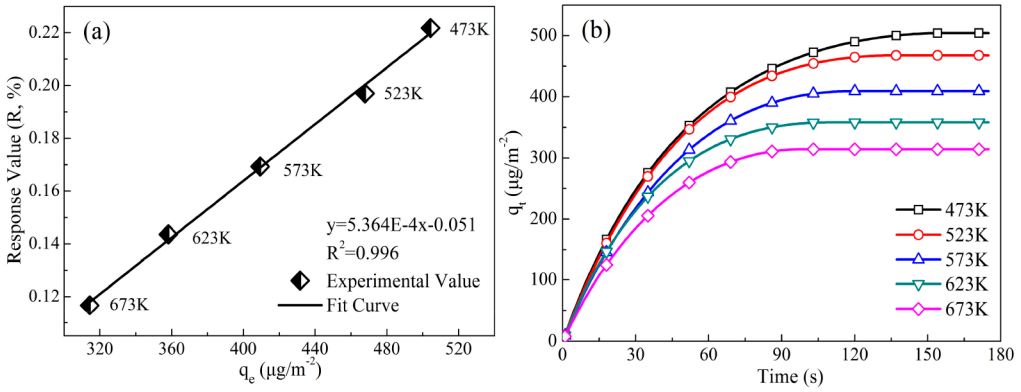

Figure 10. (a) Linear relationship between the response value of a calcite surface to CO_2 and the equilibrium amount adsorbed. (b) Amount of CO_2 adsorbed as a function of time.

process, shown in Figure 4 (starting at 600 s), was converted into the CO_2 adsorption process, as shown in Figure 10(b). When the trend of the curve was stable, the corresponding vertical axis was the equilibrium adsorption amount. An adsorption kinetic study was essential to determine the energy barrier to be overcome in gas adsorption processes and the adsorption rate. Therefore, the pseudo-first-order kinetic model was used to explore the adsorption process, which can be described as

$$\frac{dq}{dt} = k_1(q_e - q_t) \tag{2}$$

where t is the adsorption time (s), q_e is the equilibrium adsorption amount ($\mu g/m^2$), and q_t is the adsorption amount at time t. The variable k_1 is the pseudo-first-order rate constant (s^{-1}). By integrating for the boundary conditions ($t = 0$, $q = 0$; $t = t$, $q = q$), the following equation was obtained:

$$\ln(q_e - q_t) = \ln q_e - k_1 t \tag{3}$$

According to the pseudo-first-order kinetic model, the kinetic parameters were calculated and are shown in Table 1.

Table 1. Kinetic Parameters Obtained from Pseudo-First-Order Kinetic Model

T (K)	q_e ($\mu g/m^2$)[a]	q_e' ($\mu g/m^2$)[b]	k_1 (s^{-1})	R^2
473	504.3	556.6	0.0272	0.9910
523	467.8	503.4	0.0314	0.9879
573	409.3	447.0	0.0342	0.9818
623	358.1	396.6	0.0368	0.9865
673	314.3	358.3	0.0412	0.9748

[a]The variable q_e is the experimental value. [b]The variable q_e' is the model prediction value.

It was clear that the increase in temperature from 473 to 673 K brought about an increase in the adsorption rate constants k_1 and a decrease in the adsorption amount q_e. Besides, the model prediction values q_e' were very close to the experimental values q_t. A linear dependency meant a good fit between experimental results and model calculations.

After a series of adsorption rate constants, k_1, of CO_2 at different temperatures were obtained, the adsorption activation energy of CO_2 could be calculated by means of the Arrhenius equation:

$$k_1 = A \exp(-E_a/RT) \tag{4}$$

where E_a, A, and R refer to the Arrhenius activation energy, Arrhenius factor, and gas constant, respectively. Equation 4 can also be expressed as

$$\ln k_1 = \ln A - E_a/RT \tag{5}$$

According to the data in Table 1 and eq 5, the adsorption activation energy E_a can be directly calculated from the slope of the fitted curve. Figure 11 shows plots of k_1 versus the inverse

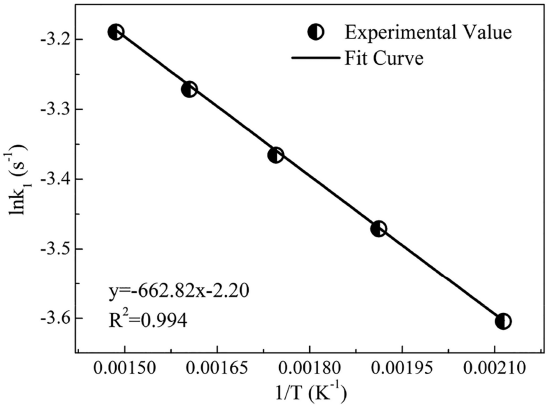

Figure 11. Linear dependence between k_1 and $1/T$ for calculating CO_2 adsorption activation energy on the calcite surface.

temperature $1/T$ in an Arrhenius-type plot. The plots were linearly fitted, with correlation coefficients R^2 greater than 0.99, showing a good linearity between k_1 and $1/T$. Therefore, the energy barrier to be overcome by the process of CO_2 adsorption on a calcite surface is available from the slope of the fitted curve, which is 5.51 kJ/mol.

3.4.2. Activation Energy Validation: MD Simulation. From the point of view of gas motion (diffusion), the main energy barrier to be overcome in CO_2 adsorption on a calcite surface was the gas diffusion energy barrier.[43−47] The diffusion activation energy can be obtained by calculating the gas motion parameters according to MD simulation,[45,48] and by this means, the energy barrier of CO_2 adsorption on a calcite surface can be well verified. Therefore, the mean-squared displacement (MSD) and diffusion coefficients (D_s) were used to investigate the diffusion properties of gases according to the Einstein diffusion law; these quantities were computed by the following equations:[49−51]

DOI: 10.1021/acs.energyfuels.9b01771
Energy Fuels 2019, 33, 8946−8953

$$\mathrm{MSD}(t) = \frac{1}{N}\sum_{i=1}^{N}\langle |r_i(t) - r_i(0)|^2\rangle \quad (6)$$

$$D_s = \frac{1}{6}\lim_{t\to\infty}\frac{\mathrm{d}}{\mathrm{d}t}\sum_{i}^{n}\langle |r_i(t) - r_i(0)|^2\rangle \quad (7)$$

where N is the number of molecules, $r_i(t)$ is the position of molecule when the time is t, and $r_i(0)$ is the initial position. According to eqs 6 and 7, the diffusion coefficients were calculated and are shown in Table 2. Clearly, the increase in temperature from 473 to 673 K brought about an increase in the diffusion coefficients D_s.

Table 2. Diffusion Coefficient of CO_2 on a Calcite Surface at Different Temperatures

T (K)	473	523	573	623	673
D_s (10^{-8} m^2/s)	2.11	2.42	2.71	2.97	3.22

After a series of the diffusion coefficients, D_s, of CO_2 at different temperatures were obtained, the diffusion activation energy of CO_2 could be calculated by means of the Arrhenius equation:

$$D_s = D_0 \exp(-E_a'/RT) \quad (8)$$

where E_a', A, and R refer to the Arrhenius activation energy, the Arrhenius factor, and gas constant, respectively. Equation 8 can also be expressed as

$$D_s = D_0 \exp(-E_a'/RT) \quad (9)$$

According to the data in Table 2 and eq 9, the diffusion activation energy E_a' could be directly calculated from the slope of the fitted curve. Figure 12 shows the Arrhenius

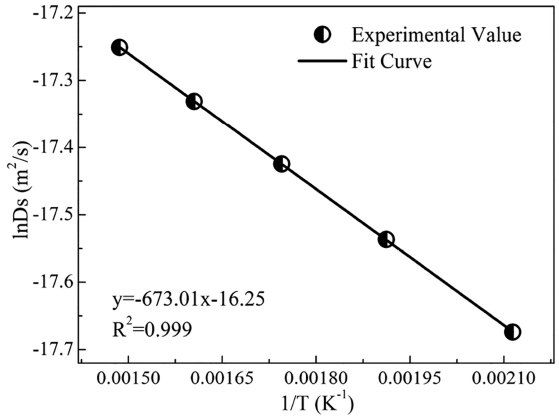

Figure 12. Linear dependence between D_s and $1/T$ for calculating CO_2 diffusion activation energy on a calcite surface.

temperature dependence of the diffusion coefficients along with the activation energy for diffusion. Therefore, the energy barrier to be overcome by the process of CO_2 diffusion to a calcite surface was available from the slope of the fitted curve, which was 5.60 kJ/mol. This result was consistent with the energy barrier obtained by the gas adsorption experiment, which indicated that at least 5.51 kJ/mol should be overcome when CO_2 was adsorbed on a calcite surface.

4. CONCLUSION

In this work, a new electrochemical method and MD simulation were used to study the adsorption kinetics of CO_2 on a reconstructed calcite (104) surface. It can be concluded that the CO_2 adsorption process can lead to a decrease in electrical conductivity and that the response value of a calcite surface to CO_2 was linearly related to temperature. With rising temperature, the degree of surface reconstruction was increased, resulting in a decrease in the band gap. In addition, when CO_2 molecules were adsorbed on the surface of calcite by electrostatic interaction, a double-layer adsorption structure was formed below 473 K. Because of the linear relationship between the response value of a calcite surface to CO_2 and the amount of CO_2 adsorbed, the process of electrical current change was the process of CO_2 adsorption. Therefore, the pseudo-first-order kinetic model was used to obtain the adsorption rate constant, which ranged from 0.0272 to 0.0412 s^{-1}. The energy barrier to be overcome in the gas adsorption process was calculated to be 5.51 kJ/mol by the Arrhenius equation. This was consistent with the results of MD simulation.

AUTHOR INFORMATION

Corresponding Authors

*E-mail: yxtaj@163.com (X.Y.). Tel.: (86) 0412-5929557. Fax: (86) 0412-5929557.
*E-mail: wangqi8822@sina.com (Q.W.).

ORCID

Lin Tao: 0000-0002-3268-7009
Qi Wang: 0000-0002-1741-2250
Zhi Li: 0000-0001-6381-5037

Notes

The authors declare no competing financial interest.

ACKNOWLEDGMENTS

The funding from the National Natural Science Foundation of China (51634004 and 51874169) and the Graduate Education Reform and Science Technology Innovation Entrepreneurship Project of University of Science and Technology Liaoning (LKDYC201801) are gratefully acknowledged.

REFERENCES

(1) Arias, J. L.; Fernández, M. a. S. Polysaccharides and proteoglycans in calcium carbonate-based biomineralization. *Chem. Rev.* **2008**, *108* (11), 4475−4482.

(2) Huijgen, W. J. J.; Comans, R. N. J. Mineral CO2 sequestration by steel slag carbonation. *Environ. Sci. Technol.* **2005**, *39* (24), 9676−9682.

(3) Sun, H.; Zhao, H.; Qi, N.; Qi, X.; Zhang, K.; Sun, W.; Li, Y. Mechanistic insight into the displacement of CH4 by CO2 in calcite slit nanopores: the effect of competitive adsorption. *RSC Adv.* **2016**, *6* (106), 104456−104462.

(4) Santos, M. S.; Franco, L. F. M.; Castier, M.; Economou, I. G. Molecular Dynamics Simulation of n-Alkanes and CO2 Confined by Calcite Nanopores. *Energy Fuels* **2018**, *32* (2), 1934−1941.

(5) Sun, H.; Zhao, H.; Qi, N.; Zhang, X.; Li, Y. Exploration of Capturing CO2 from Flue Gas by Calcite Slit-Nanopores: A Computational Investigation. *Energy Technology* **2018**, *6*, 1732.

(6) Ma, Y.; Lu, G.; Shao, C.; Li, X. Molecular dynamics simulation of hydrocarbon molecule adsorption on kaolinite (0 0 1) surface. *Fuel* **2019**, *237*, 989−1002.

DOI: 10.1021/acs.energyfuels.9b01771
Energy Fuels 2019, 33, 8946−8953

(7) Jiang, H.; Economou, I. G.; Panagiotopoulos, A. Z. Molecular Modeling of Thermodynamic and Transport Properties for CO2 and Aqueous Brines. *Acc. Chem. Res.* **2017**, *50* (4), 751−758.
(8) Wang, S.; Zhou, G.; Ma, Y.; Gao, L.; Song, R.; Jiang, G.; Lu, G. Molecular dynamics investigation on the adsorption behaviors of H2O, CO2, CH4 and N2 gases on calcite (1 $\bar{1}$ 0) surface. *Appl. Surf. Sci.* **2016**, *385*, 616−621.
(9) Sun, H.; Zhao, H.; Qi, N.; Li, Y. Effects of Surface Composition on the Microbehaviors of CH4 and CO2 in Slit-Nanopores: A Simulation Exploration. *ACS Omega* **2017**, *2* (11), 7600−7608.
(10) Franco, L. F.; Castier, M.; Economou, I. G. Anisotropic parallel self-diffusion coefficients near the calcite surface: A molecular dynamics study. *J. Chem. Phys.* **2016**, *145* (8), 084702.
(11) Tao, L.; Li, Z.; Wang, G.-C.; Cui, B.-Y.; Yin, X.-T.; Wang, Q. Evolution of calcite surface reconstruction and interface adsorption of calcite-CO2 with temperature. *Mater. Res. Express* **2019**, *6* (2), 025035.
(12) Lu, X.; Jin, D.; Wei, S.; Zhang, M.; Zhu, Q.; Shi, X.; Deng, Z.; Guo, W.; Shen, W. Competitive adsorption of a binary CO 2−CH 4 mixture in nanoporous carbons: effects of edge-functionalization. *Nanoscale* **2015**, *7* (3), 1002−1012.
(13) Wang, X.; Qin, H.; Chen, Y.; Hu, J. Sensing mechanism of SnO2 (110) surface to CO: density functional theory calculations. *J. Phys. Chem. C* **2014**, *118* (49), 28548−28561.
(14) Zeng, W.; Liu, T.; Liu, D.; Han, E. Hydrogen sensing and mechanism of M-doped SnO2 (M= Cr3+, Cu2+ and Pd2+) nanocomposite. *Sens. Actuators, B* **2011**, *160* (1), 455−462.
(15) Yin, X.-T.; Guo, X.-M. Selectivity and sensitivity of Pd-loaded and Fe-doped SnO2 sensor for CO detection. *Sens. Actuators, B* **2014**, *200*, 213−218.
(16) Yin, X.-T.; Tao, L. Fabrication and gas sensing properties of Au-loaded SnO2 composite nanoparticles for low concentration hydrogen. *J. Alloys Compd.* **2017**, *727*, 254−259.
(17) Liu, T.; Wang, X.; Zhang, X.; Gao, X.; Li, L.; Yu, J.; Yin, X. A limiting current oxygen sensor prepared by a co-pressing and co-sintering technique. *Sens. Actuators, B* **2018**, *277*, 216−223.
(18) Wang, S.; Feng, Q.; Javadpour, F.; Yang, Y. Breakdown of Fast Mass Transport of Methane through Calcite Nanopores. *J. Phys. Chem. C* **2016**, *120* (26), 14260−14269.
(19) Gao, Z.; Li, C.; Sun, W.; Hu, Y. Anisotropic surface properties of calcite: A consideration of surface broken bonds. *Colloids Surf., A* **2017**, *520*, 53−61.
(20) Kerisit, S.; Parker, S. C.; Harding, J. H. Atomistic simulation of the dissociative adsorption of water on calcite surfaces. *J. Phys. Chem. B* **2003**, *107* (31), 7676−7682.
(21) Rodriguez-Navarro, C.; Ruiz-Agudo, E.; Luque, A.; Rodriguez-Navarro, A. B.; Ortega-Huertas, M. Thermal decomposition of calcite: Mechanisms of formation and textural evolution of CaO nanocrystals. *Am. Mineral.* **2009**, *94* (4), 578−593.
(22) Rohl, A. L.; Wright, K.; Gale, J. D. Evidence from surface phonons for the (2× 1) reconstruction of the (1014) surface of calcite from computer simulation. *Am. Mineral.* **2003**, *88* (5−6), 921−925.
(23) Javanbakht, G.; Sedghi, M.; Welch, W.; Goual, L. Molecular dynamics simulations of CO2/water/quartz interfacial properties: Impact of CO2 dissolution in water. *Langmuir* **2015**, *31* (21), 5812−5819.
(24) Zhang, L.; Hu, Z.; Jiang, J. Metal−Organic Framework/Polymer Mixed-Matrix Membranes for H2/CO2 Separation: A Fully Atomistic Simulation Study. *J. Phys. Chem. C* **2012**, *116* (36), 19268−19277.
(25) Zhuo, S.; Huang, Y.; Hu, J.; Liu, H.; Hu, Y.; Jiang, J. Computer Simulation for Adsorption of CO2, N2and Flue Gas in a Mimetic MCM-41. *J. Phys. Chem. C* **2008**, *112* (30), 11295−11300.
(26) Potoff, J. J.; Siepmann, J. I. Vapor−liquid equilibria of mixtures containing alkanes, carbon dioxide, and nitrogen. *AIChE J.* **2001**, *47* (7), 1676−1682.
(27) Delley, B. An all-electron numerical method for solving the local density functional for polyatomic molecules. *J. Chem. Phys.* **1990**, *92* (1), 508−517.
(28) Delley, B. From molecules to solids with the DMol 3 approach. *J. Chem. Phys.* **2000**, *113* (18), 7756−7764.
(29) Perdew, J. P.; Burke, K.; Ernzerhof, M. Generalized gradient approximation made simple. *Phys. Rev. Lett.* **1996**, *77* (18), 3865.
(30) Perdew, J. P.; Burke, K.; Wang, Y. Generalized gradient approximation for the exchange-correlation hole of a many-electron system. *Phys. Rev. B: Condens. Matter Mater. Phys.* **1996**, *54* (23), 16533.
(31) Sun, H. COMPASS: an ab initio force-field optimized for condensed-phase applications overview with details on alkane and benzene compounds. *J. Phys. Chem. B* **1998**, *102* (38), 7338−7364.
(32) Sun, H.; Ren, P.; Fried, J. The COMPASS force field: parameterization and validation for phosphazenes. *Comput. Theor. Polym. Sci.* **1998**, *8* (1−2), 229−246.
(33) Wang, Y.; Yang, Q.; Li, J.; Yang, J.; Zhong, C. Exploration of nanoporous graphene membranes for the separation of N2 from CO2: a multi-scale computational study. *Phys. Chem. Chem. Phys.* **2016**, *18* (12), 8352−8.
(34) Ataman, E.; Andersson, M. P.; Ceccato, M.; Bovet, N.; Stipp, S. L. S. Functional group adsorption on calcite: I. Oxygen containing and nonpolar organic molecules. *J. Phys. Chem. C* **2016**, *120* (30), 16586−16596.
(35) Baer, D.; Blanchard, D. L., Jr Studies of the calcite cleavage surface for comparison with calculation. *Appl. Surf. Sci.* **1993**, *72* (4), 295−300.
(36) Mirwald, P. W. The electrical conductivity of calcite between 300 and 1200 C at a CO 2 pressure of 40 bar. *Phys. Chem. Miner.* **1979**, *4* (4), 291−297.
(37) Fenter, P.; Sturchio, N. Calcite (1 0 4)−water interface structure, revisited. *Geochim. Cosmochim. Acta* **2012**, *97*, 58−69.
(38) Geysermans, P.; Noguera, C. Advances in atomistic simulations of mineral surfaces. *J. Mater. Chem.* **2009**, *19* (42), 7807−7821.
(39) Pacchioni, G. Surface reconstructions: Polaron bricklayers at work. *Nature Reviews Materials* **2017**, *2* (11), 17071.
(40) Oura, K.; Lifshits, V.; Saranin, A.; Zotov, A.; Katayama, M. *Surface science: an introduction* **2003**, 1.
(41) Diebold, U. Oxide surfaces: Surface science goes inorganic. *Nat. Mater.* **2010**, *9* (3), 185.
(42) Allara, D. L. A perspective on surfaces and interfaces. *Nature* **2005**, *437* (7059), 638−639.
(43) Zhao, Z.; Li, Z.; Lin, Y. S. Adsorption and Diffusion of Carbon Dioxide on Metal-Organic Framework (MOF-5). *Ind. Eng. Chem. Res.* **2009**, *48* (22), 10015−10020.
(44) Zhang, Z.; Huang, S.; Xian, S.; Xi, H.; Li, Z. Adsorption equilibrium and kinetics of CO2 on chromium terephthalate MIL-101. *Energy Fuels* **2011**, *25* (2), 835−842.
(45) Gao, M.; Khalkhali, M.; Beck, S.; Choi, P.; Zhang, H. Study of Thermal Stability of Hydrotalcite and Carbon Dioxide Adsorption Behavior on Hydrotalcite-Derived Mixed Oxides Using Atomistic Simulations. *ACS Omega* **2018**, *3* (9), 12041−12051.
(46) Yucel, H.; Ruthven, D. M. Diffusion of CO2 in 4A and 5A zeolite crystals. *J. Colloid Interface Sci.* **1980**, *74* (1), 186−195.
(47) Shelekhin, A. B.; Dixon, A. G.; Ma, Y. H. Theory of gas diffusion and permeation in inorganic molecular-sieve membranes. *AIChE J.* **1995**, *41* (1), 58−67.
(48) Skoulidas, A. I.; Sholl, D. S. Self-diffusion and transport diffusion of light gases in metal-organic framework materials assessed using molecular dynamics simulations. *J. Phys. Chem. B* **2005**, *109* (33), 15760−8.
(49) Zhai, Z.; Wang, X.; Jin, X.; Sun, L.; Li, J.; Cao, D. Adsorption and diffusion of shale gas reservoirs in modeled clay minerals at different geological depths. *Energy Fuels* **2014**, *28* (12), 7467−7473.
(50) Wu, G.; Zhu, X.; Ji, H.; Chen, D. Molecular modeling of interactions between heavy crude oil and the soil organic matter coated quartz surface. *Chemosphere* **2015**, *119*, 242−249.
(51) Einstein, A. On the movement of small particles suspended in stationary liquids required by the molecularkinetic theory of heat. *Ann. Phys.* **1905**, *322*, 549−560.

DOI: 10.1021/acs.energyfuels.9b01771
Energy Fuels 2019, 33, 8946−8953